Preliminary Fuel Cycle Analysis of the -UB_2 Composite Fuels in Pressurized Water Reactors

Zeyun Wu† and Cihang Lu*

Department of Mechanical and Nuclear Engineering, Virginia Commonwealth University, Richmond VA 23284

†Corresponding author: zwu@vcu.edu

doi.org/10.13182/T126-38212

INTRODUCTION

Burnable absorbers (BA) are being commonly employed in operating pressurized water reactor (PWR) to hold down the excess reactivity in the early stage of the fuel cycles. Due to the large $^{10}B(n,\alpha)^7Li$ cross section in the thermal range, boron is a common BA employed in forms of soluble boric acid dissolved in the coolant, the concentration of which keeps being adjusted to keep the reactor critical. The Wet Annular Burnable Absorber (WABA) [1] and the Integral Fuel Burnable Absorber (IFBA) [2] are two alternative BA forms invented by Westinghouse. The WABA consists of annular pellets of alumina-boron carbide (Al_2O_3-B_4C) contained within two concentric Zircaloy-4 [3] tubes. WABA has one drawback that the BA rods displace fuel rods from the fuel assembly, which results in reduced heavy metal (HM) loading and shorter fuel cycles. This defect can be circumvented via the use of the IFBA, which consists of coatings of thin layers of zirconium diboride (ZrB_2) over the outer surfaces of the conventional UO_2 fuel pellets. However, the IFBA has its own limitations. For example, while enormous efforts have been made to enhance the thermal conductivity of the nuclear fuel in the aftermath of the 2011 Fukushima disaster, adding a coating material to the surface of the fuel rod inevitability worsens the heat transfer between the fuel and the coolant, which results in a higher fuel center-line temperature. Also, the coating may lead to early burn out of the BA and induce undesirable reactivity peaks [4], which also increases the fuel temperature.

In the light of the above limitations, several novel composite fuels with uranium diboride (UB_2) as the secondary phase have been proposed to improve both the safety and the economic performances of the PWR [5, 6]. Three of these composite fuels, namely the UO_2-UB_2, U_3Si_2-UB_2, and UN-UB_2, were investigated in this work. U_3Si_2, UN, and UB_2, as the primary ingredients of the composite fuels, all have enhanced HM loadings (9.68 g-U/cm^3 for UO_2, 11.68 g-U/cm^3 for UB_2, 11.3 U/cm^3 for U_3Si_2, and 13.35 g-U/cm^3 for UN). Additional advantages of these composite fuels include:

- These composite fuels have higher thermal conductivities than the conventional UO_2 fuel, which limits the fuel temperature.
- By appropriately adjusting the $^{10}B/^{11}B$ ratio, the -UB_2 fuels also function as the BA. The more distributed BA in fuel rods, instead of the several dedicated BA rods, decreases the power peaking factor and therefore the peak fuel temperature.
- The use of these composite fuels avoids the potential early burnout of the BA coatings.

All the above merits of the -UB_2 composite fuels undoubtably improve the safety of a PWR.

This paper analyzed, on the other hand, the economic viability of these -UB_2 composite fuels via fuel cycle analyses, as a longer fuel cycle length implies less frequent refueling outages, which leads to a higher availability and more profit. While UO_2-UB_2 and U_3Si_2-UB_2 have been recently fabricated in the laboratory environment, no production of the UN-UB_2 composite has been reported. This work therefore also makes suggestions for the focus of potential future experiments on UN-UB_2.

COMPUTTATIONAL MODELS

PWR Fuel Assembly

The Westinghouse's AP-1000 reactor was considered as the reference design in this work, and the 17 x 17 fuel assembly was modeled according to its specifications [7]. Important parameters of the fuel assembly are summarized in TABLE I. The mass density of the Zircaloy-4 cladding was 5.78 g/cm^3 [8]. The coolant with a boron concentration of 500 ppm had a mass density of 0.719 g/cm^3 [9]. The stochastic neutronics tool Serpent [10] was used for the modeling work, and the ENDF/B-VII.0 library was employed. The fuel materials were modeled at 900 K, while the non-fuel materials were modeled at 600 K. The 2-D fuel assembly model is shown in Fig. 1.

TABLE I. Specifications of fuel assembly.

Parameter	Value
Array size (-)	17 x 17
Number of fuel rods (-)	264
Number of guide/instrument tubes (-)	25
Power density (MW/MTU)	40.2
Rod pitch (cm)	1.26
Assembly pitch (cm)	21.522
Cladding outside radius (cm)	0.475
Gas gap outside radius (cm)	0.4178
Pellet outside radius (cm)	0.4096
Guide/instrument tube outside radius (cm)	0.6121
Guide/instrument tube inside radius (cm)	0.5715

* Current address: Nuclear Science & Technology Department, Brookhaven National Laboratory (clu@bnl.gov)

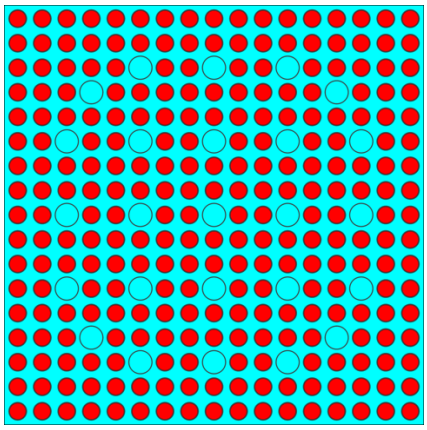

Fig. 1. The 2-D Serpent model of the 17 x 17 fuel assembly.

Loading patterns with 0, 8, 16, 32, 48, 64, 80, 104, 128, and 156 IFBA rods are known to exist for a Westinghouse 17 × 17 assembly [8]. We considered the bounding cases and compared the fuel cycle performance of the three composite fuels with conventional UO_2 assemblies with 0 and 156 IFBA rods. The loading pattern for the 156 IFBA rods is shown in Fig. 2. Natural boron was considered for both the soluble boric acid and the ZrB_2 coating of the IFBA rods. We assumed 1.57 mg/inch of ^{10}B in the IFBA rods [8], where the thickness of the ZrB_2 coating was 0.000508 cm [11]. An initial ^{235}U enrichment of 3.4 wt.%, which is one of the typical initial enrichments in the AP-100 design, was assumed for all the fuels in this study, including the conventional UO_2 fuel and the three composite fuels.

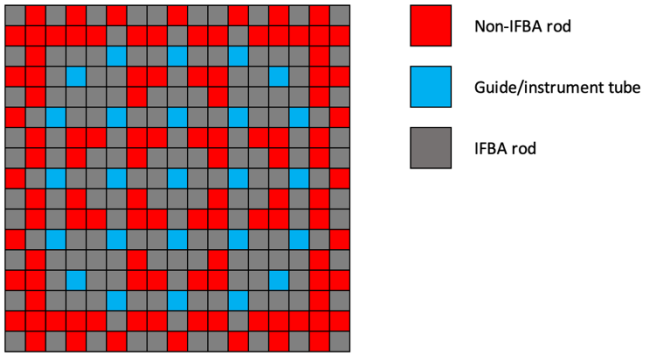

Fig. 2. Loading pattern of the 156 IFBA rods.

The UO_2-UB_2 Composite

The UO_2-UB_2 composites, with UB_2 phase fractions of 5 wt.%, 15 wt.%, and 30 wt.%, were recently fabricated at Las Alamos National Laboratory [5]. The composites were fabricated to high densities (> 95% theoretical density) via spark plasma sintering (SPS). The use of the UO_2 as the primary phase aids from a regulatory and fabrication infrastructure standpoint, while the incorporation of the UB_2 as the secondary phase improves both the overall thermal conductivity and fissile density [5]. It is pointed out that UO_2-UB_4 was also fabricated. However, because of the significantly lower HM density of UB_4 (13.35 g-U/cm^3), UO_2-UB_4 was not considered in this work.

The UO_2-UB_2 composites were modeled with 30 wt.% of UB_2 in this work with 95% theoretical densities. The ^{10}B concentration was varied to study its impact on the fuel cycle performance. At room temperature, the theoretical density of UO_2 and UB_2 are 10.97 g/cm^3 and 12.7 g/cm^3, respectively [12]. We assumed this ratio in theoretical mass density unchanged at 900 K and calculated the theoretical density of UB_2 to be 11.84 g/cm^3, as UO_2 has a theoretical density of 10.766 g/cm^3 at 900 K [13].

The U_3Si_2-UB_2 Composite

The U_3Si_2-UB_2 composite, with 0 - 100% UB_2 phase fractions, were recently fabricated in the University of Manchester via arc melting, followed by cold pressing and sintering. The density of the composite was measured to be similar to the reference U_3Si_2 material [6]. Unlike the UO_2-UB_2 composites, the U_3Si_2-UB_2 composite was not expected to increase the fuel cycle length of U_3Si_2, viewing the comparable HM densities of both materials. The UB_2 was added as the secondary phase to U_3Si_2 such that the later can be less reactant to the high-pressure steam. It was found that the addition of 10 wt.% of UB_2 to U_3Si_2 increases the onset temperature of the steam reaction by around 100 K, and the addition of 50 wt. % UB_2 maintains this increase [6].

The U_3Si_2-UB_2 composite were modeled with 30 wt.% of UB_2 in this work with 95% theoretical densities. The ^{10}B concentration was varied to study its impact on the fuel cycle performance. At room temperature, the theoretical density of U_3Si_2 is 12.2 g/cm^3 [14]. The theoretical density of U_3Si_2 was calculated to be 11.37 g/cm^3 at 900 K in the same way as the UB_2.

The UN-UB_2 Composite

No fabrication of the UN-UB_2 composite has been reported yet. Similar to the U_3Si_2-UB_2 composite, the UB_2 is a desirable secondary phase to UN to mitigate its reaction with high-pressure steam. One uniqueness of the UN-UB_2 composite is that natural nitrogen contains 99.6 at.% of ^{14}N, which has a relatively strong neutron absorption cross-section for the $^{14}N(n,p)^{14}C$ reaction in the thermal energy range [9].

The UN-UB_2 composite were modeled with 30 wt.% of UB_2 in this work with 95% theoretical densities. Both the ^{10}B and ^{14}N concentrations were varied to study their impact on the fuel cycle performance. The theoretical density of UN is 14.13 g/cm^3 at 900 K [15].

RESULTS

The impact of the composite fuels on the infinite multiplication factor and the fuel cycle length, expressed in effective full power days (EFPD), is shown in Fig. 3 in comparison with the bounding reference 0- and 156-IFBA-rods cases. All the three composite fuels were able to increase the fuel cycle length of the 0-IFBA-rods assembly when

employing 100% enriched ^{11}B and ^{15}N, thanks to the enhanced HM loadings, as summarized in TABLE II. It is noted that the HM loading in TABLE II. is per assembly with a thickness of 1 cm. Fig. 3 also demonstrated that by appropriately adjusting the ^{10}B concentration of the composite fuels, they are capable to function similarly to the 156-IFBA-rods assemblies for the holding down of the initial excess reactivity.

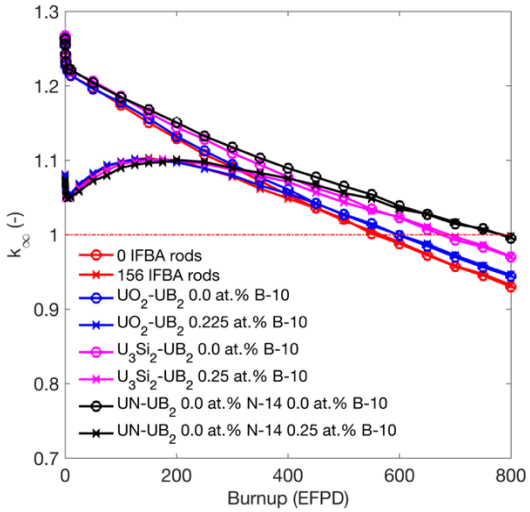

Fig. 3. Comparison of the k_∞ as a function of EFPD of the various composite fuels.

TABLE II. Summary of fuel cycle length and HM loadings.

Fuel type	EFPD	+	HM loading (g)	+
0-IFBA	556	-	1254	-
UO_2-UB_2	597	7%	1323	5%
U_3Si_2-UB_2	675	21%	1479	18%
UN-UB_2	782	41%	1680	34%

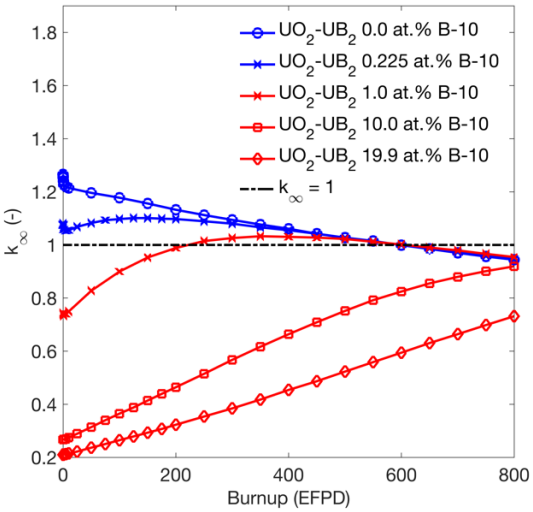

Fig. 4. Impact of ^{10}B concentration on k_∞ for UO_2-UB_2.

Although all these composite fuels, with appropriate ^{10}B concentrations, can help hold down the excess reactivity at the early stage of the cycle, the penalty on the initial reactivity may soon become unacceptable with an increasing ^{10}B concentrations. The impact of the ^{10}B concentration on the infinite multiplication factor is shown in Fig. 4-6 respectively for UO_2-UB_2, U_3Si_2-UB_2, and UN-UB_2 fuels.

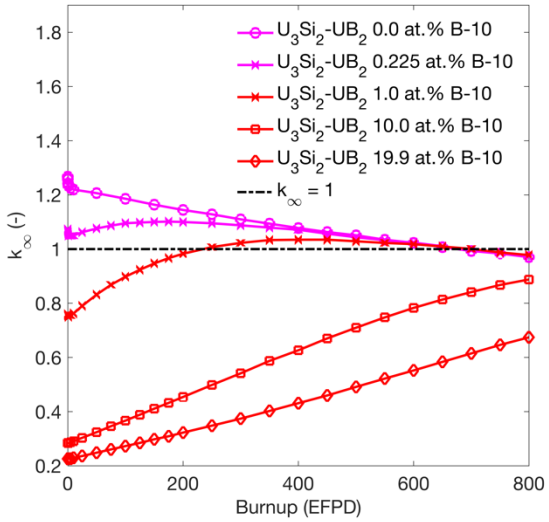

Fig. 5. Impact of ^{10}B concentration on k_∞ for U_3Si_2-UB_2.

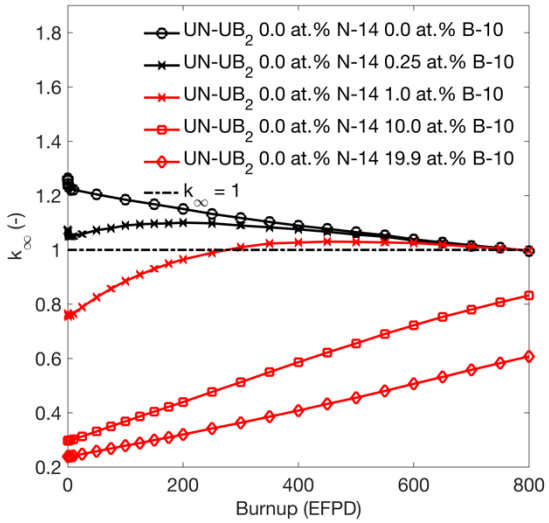

Fig. 6. Impact of ^{10}B concentration on k_∞ for UN-UB_2.

For all the three composite fuels, a ^{10}B concentration of a few 0.1 at.% will be reasonable, while the employment of natural boron (which has a ^{10}B concentration of a 19.9 at.%) would be impractical. The enrichment of ^{11}B to a large extent (~99.9 at.%) may be costly and not worth the increased fuel cycle length brought by the employment of the -UB_2 composite fuels.

The impact of the ^{14}N concentration of UN-UB_2 on the infinite multiplication factor, as shown in Fig. 7, is less significant compared to ^{10}B. This is because of the relatively smaller neutron absorption cross section of ^{14}N in the thermal

range [16], as shown in Fig. 8. However, when natural nitrogen (which has a ^{14}N concentration of a 99.6 at.%) is employed, the increase in the fuel cycle length brought by the enhanced HM loading of UN is canceled out.

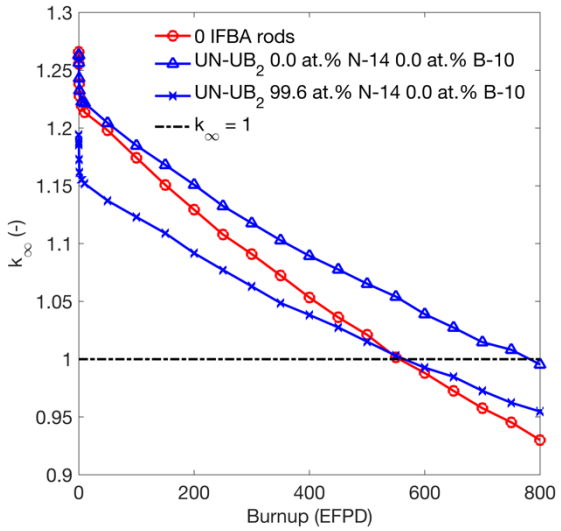

Fig. 7. Impact of ^{14}N concentration on k_∞ for UN-UB_2.

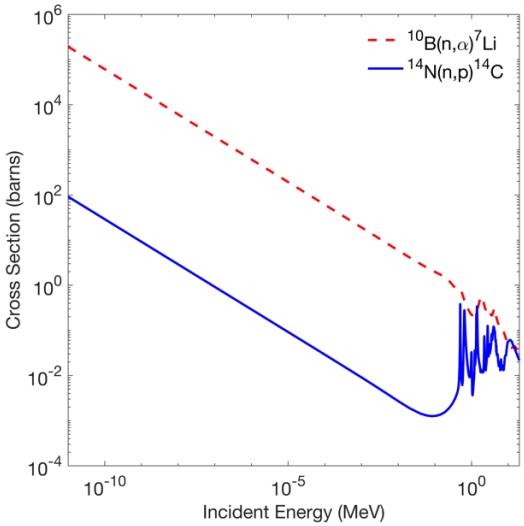

Fig. 8. Comparison of ^{14}N and ^{10}B absorption cross section.

CONCLUSIONS

All the calculations in this work were performed by assuming 30 wt.% of the UB_2 phase in the composite fuels. The results indicate the impact of the ^{10}B concentration on the reactivity decreases with a smaller amount of UB_2. However, a significant amount of UB_2 is required in the UO_2-UB_2 composite to achieve a higher HM loading for an extended fuel cycle length. In contrast, UB_2 is added to U_3Si_2 and UN primarily to make them less reactant with high-pressure steam, rather than to increase the HM loading. Therefore, in future work, the minimum amount of UB_2 required to adequately mitigate the UN-steam reaction should be experimentally determined.

REFERENCES

1. Westinghouse Electric Company LLC, "Nuclear fuel - Wet Annular Burnable Absorber (WABA) assembly," NFCM-0016 (2017).
2. Westinghouse Electric Company LLC, "Nuclear fuel - Integral Fuel Burnable Absorber (IFBA) fuel cycles and IFBA/Gad hybrid fuel cycles," NFCM-0015 (2018).
3. C. WHITMARSH, "Review of Zircaloy-2 and Zircaloy-4 properties relevant to N.S. Savannah," (1962)
4. F. FRANCESCHINI and B. PETROVIC, "Fuel with advanced burnable absorbers design for the IRIS reactor core: combined Erbia and IFBA," *Annals of Nuclear Energy*, **36**, 1201–1207 (2009).
5. KARDOULAKI et al., "Fabrication and thermophysical properties of UO_2-UB_2 and UO_2-UB_4 composites sintered via spark plasma sintering," *Journal of Nuclear Materials*, **544**, 152690 (2021).
6. J. TURNER and T. ABRAM, "Steam performance of UB_2/U_3Si_2 composite fuel pellets, compared to U_3Si_2 reference behaviour," *Journal of Nuclear Materials*, **529**, 151919 (2020).
7. Westinghouse Electric Company LLC, "AP1000 European Design Control Document," (2009).
8. C. SANDERS and J. WAGNER, "Study of the effect of Integral Burnable Absorbers for PWR burnup credit," NUREG/CR-6760, ORNL/TM-2000/321 (2002).
9. N. BROWN et al., "Neutronic performance of uranium nitride composite fuels in a PWR," *Nuclear Engineering and Design*, **275**, 393–407 (2014).
10. J. LEPPANEN, "The Serpent Monte Carlo code: status, development and applications in 2013," *Annals of Nuclear Energy*, **82**, 142–150 (2015).
11. F. FRANCESCHINI et al., "Westinghouse VERA test stand zero power physics test simulations for the AP1000 PWR," CASL-U-2014-0012-000 (2014).
12. W. HAYNES, et al., *CRC Handbook of Chemistry and Physics: A Ready-Reference Book of Chemical and Physical Data*, 97th Edition, CRC Press (2017).
13. S. POPOV et al., "Thermophysical properties of MOX and UO2 fuels including the effects of irradiation," ORNL/TM-2000/351 (2000).
14. K. METZGER et al., "Model of U_3Si_2 fuel system using BISON fuel code," INL/CON-13-30445 (2014).
15. S. L. HAYES et al., "Material property correlations for uranium mononitride," *Journal of Nuclear Materials*, **171**, 262-170 (1990).
16. D. B. BROWN et al., "ENDF/B-VIII.0: The 8th major release of the nuclear reaction data library with CIELO-project cross sections, new standards and thermal scattering data," *Nuclear Data Sheets*, **148**, 1-142 (2018).